JOURNAL OF OPTOELECTRONICS AND ADVANCED MATERIALS, Vol. 11, No. 11, November 2009, p. 1567 - 1575

Compositional structure analysis of thin film magnetic recording media

MASAAKI FUTAMOTO
Faculty of Science and Engineering, Chuo University, 1-13-27 Kasuga, Bunkyo-ku, Tokyo 112-8551, Japan

Magnetic and recording characteristics depend strongly on the structural and compositional microstructure of thin film media. Transmission electron microscopy (TEM) has been used to investigate the microstructure. When a chemical analysis equipment using electron energy loss spectroscopy (EELS) or energy dispersive X-ray spectroscopy (EDX) was combined with the TEM technology, it became possible to study both the detailed compositional and the structural information for a same observation area under a high-magnification condition. The present paper briefly reviews the applications of such TEM technology equipped with EELS or EDX covering the research works reported from middle 80's to the present. Examples of nm-level chemical analysis are shown for various Co-alloy thin films including a current CoCrPt-oxide granular-type perpendicular medium which consists of Co-alloy magnetic crystals of sub-10nm in diameter separated by nonmagnetic amorphous grain boundaries.

(Received October 1, 2009; accepted November 12, 2009)

Keywords: Thin film recording media, Single crystal film, Composition, Microstructure, TEM, EDX, EELS, Segregation

1. Introduction

Magnetic and recording characteristics depend strongly on the structural and compositional microstructure of thin film media. Co-alloy thin films have been employed as recording media of commercial hard disk drives (HDD). The alloy composition, the thickness, the underlayer, the deposition condition, etc. have been continuously improved to cope with the areal density increase of HDD for more than 30 years. When CoCr-alloy thin films were studied as recording media in early '80s, the saturation magnetization *(M_s)* of thin film was noted to be larger than that of bulk alloy material and the M_s varied also depending on the process condition. By considering the Co-Cr phase diagram, Cr segregation around the crystal grain boundaries and/or within crystal grains were proposed to explain the difference [1.2]. In order to investigate the compositional microstructure, selective chemical etching techniques combined with transmission electron microscopy (TEM) or scanning electron microscopy were applied to CoCr-alloy thin films [3-6]. Fig. 1 shows the TEM picture reported by Maeda et al showing "Chrysanthemum-like Pattern" observed for a Co-18at%Co film sputter deposited at 150 C, where bright and dark contrast regions correspond to Co-enriched and Cr-enriched regions, respectively [5]. Co enriched regions in the film were removed preferentially by selective chemical etching of Co. Strong chemical segregation in CoCr-alloy thin films were also confirmed by spin echo ^{59}Co nuclear magnetic resonance analysis [5, 7]. Cr segregation in CoCr-alloy thin film was started to be recognized as a strong parameter to control the microstructure and the magnetic properties.

Direct observation of compositional microstructure became possible by using a TEM equipped with a chemical analysis facility. In middle to late '80s, Chapman et al investigated the local compositional variations for plan-view CoCr-alloy thin film samples using a focused electron beam combined with an energy dispersive X-ray spectrometer (EDX) [8,9]. They observed inhomogeneity of a CoCr-alloy layer in the lateral direction induced by segregation, and concluded that the film is enriched in Co in some areas and thus has a higher local *Ms*, while other regions are Cr enriched and probably non-magnetic.

In middle '90s, Kimoto and Futamoto et al reported the detailed compositional segregation structures of CoCrTa thin film media obtained by using a field emission TEM equipped with an imaging filter [10-16]. Energy filtered images and electron energy loss spectra could be observed by using an electron energy loss spectrometer (EELS). Co and Cr atom distribution intensities were quantitatively visualized in the corresponding TEM micrographs. By using the technique, the local distributions of alloy elements have been studied for various thin film media, including CoCrPt-oxide perpendicular thin films which are employed in the current commercial HDDs with 100 – 200 Gb/in^2 areal densities [17, 18].

The TEM equipped with an EDX analysis technique has been applied from middle '90s to early 2000s to investigate the compositional microstructure of CoCr-alloy media; CoCrTa, CoCrPt, CoCrPtTa longitudinal media [12, 19-24], and recently for CoCrPt-SiO_x perpendicular media [25, 26]. This technique has also been applied to investigate the compositional distribution of magnetic thin films with bi-crystalline and single-crystal structures [23, 27, 28]. Understanding the local compositions of thin film recording media by high-resolution compositional analyses makes it possible to discuss the magnetic properties based on individual magnetic crystalline grains that form the recording media.

In the present paper, the progress of compositional analysis on magnetic thin films using TEM based technologies are briefly reviewed focusing on the data reported from the Hitachi group where the author has worked until recently.

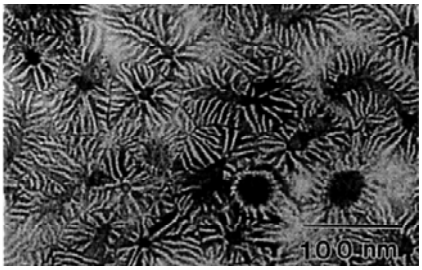

Fig. 1. TEM micrograph showing the "Crysanthemum-like pattern" structure in a sputter deposited Co-18at% Cr thin film [3].

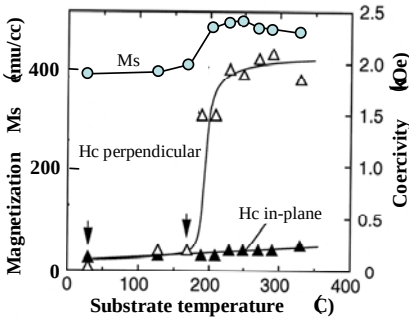

Fig. 2. Relationship between magnetic properties and substrate temperature for a Co-17at%Cr-3at%Ta perpendicular thin film media [11, 12].

2. Compositional analysis by TEM equipped with EELS

The magnetic properties of thin film media vary depending on the substrate temperature. Such an example studied for 100 nm-thick Co-13at%Cr-3at%Ta perpendicular thin film media sputter deposited on Ti underlayer is shown in Fig. 2 [11, 12]. The M_s and the coercivity (H_c) start to increase when the substrate temperature exceeds 170 C. The plan-view TEM, the Cr, and the Co mapping images observed for a sample deposited at 230 C by using a TEM equipped with an imaging filter are shown respectively in Fig. 3 (a), (b), and (c) [11,12]. These images are obtained from a same sample area and thus it is possible to map the Cr/Co ratio image calculated from the original data. The Cr/Co ratio images are compared in Fig. 4 together with the respective plan-view images for the samples prepared employing different substrate temperatures. The bright contrast corresponds to the region with Cr-enriched while the dark contrast shows the region with Co-enriched region. Compositional inhomogeneity is apparently enhanced with increasing the substrate temperature for sputter deposition. Cr atoms are strongly segregated along the grain boundaries for the sample deposited at 230 C. Quantitative compositional analysis is carried out for respective samples along the lines indicated in the micrographs [11, 15]. The results are compared in Fig. 5, where Cr contents at grain boundaries are exceeding 25 at% for the sample prepared at 230 C. When the Cr content is greater than 25 at% in Co-Cr alloy system, that region is nonmagnetic at room temperature. The data shows that a very thin nonmagnetic layer is playing a roll to magnetically separate the neighboring magnetic crystal grains, which can be related to the increase of H_c and the reduction of medium noise [13].

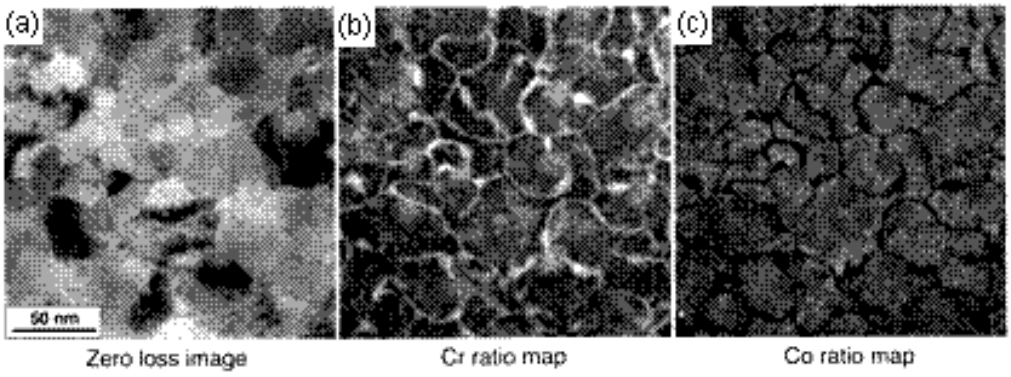

Fig. 3. Plan-view TEM (a) elemental distribution maps of Cr (b) and Co (c) observed for a CoCrTa perpendicular medium deposited at 230 ^{o}C [11, 12].

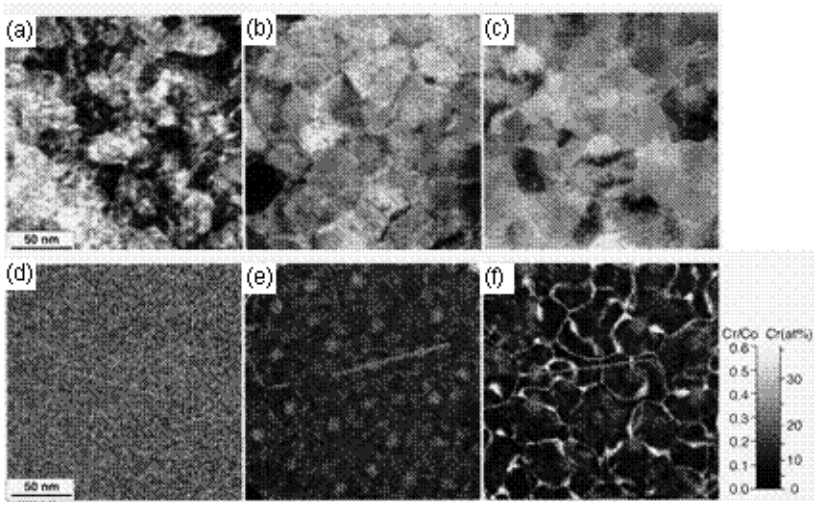

Fig. 4. Plan-view TEM images of Co-17at%Cr-3at%Ta media deposited at 20 °C (a) 170 °C (b) 230 °C (c) and the respective Cr/Co composition images (d) – (f) [11, 12, 13].

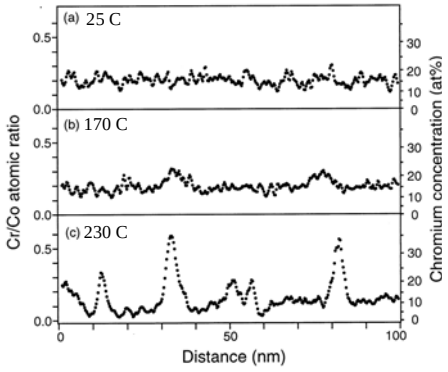

Fig. 5. Cr/Co atomic radio profiles measured for Co-17at%Cr-3at%Ta media along the lines shown in Fig. 4 [11, 12].

Examples of compositional mapping carried out for a 25 nm-thick Co-15at%Cr-4at%Ta longitudinal medium sputter deposited at 300 C on a 25 nm-thick Cr-10at%Ti underlayer are shown in Fig. 6 [16]. Similar to the case of perpendicular recording medium, Cr atoms are preferentially segregated along the grain boundaries. The compositional structures observed for a cross-sectional view of the same sample are shown in Fig. 7. Here, however, clear elements' segregation can not be recognized because of overlapping the signals along the sample thickness direction. A careful comparison between the TEM image of Fig. 7(a) and the Cr image of (b) suggests preferential Cr segregation along the columnar boundaries of CoCrTa layer. Similar results are reported from an other research group on CoCrTa longitudinal media [17]. Compositional analysis on granular CoPt-TiO_2 media are carried out using a similar technique and clear mappings of Co, O, and Ti are reported recently [18]. The TEM equipped with EELS is very powerful to investigate the detailed compositional microstructure of magnetic thin films especially including light elements like oxygen which is a very important component for recent granular-type perpendicular recording media.

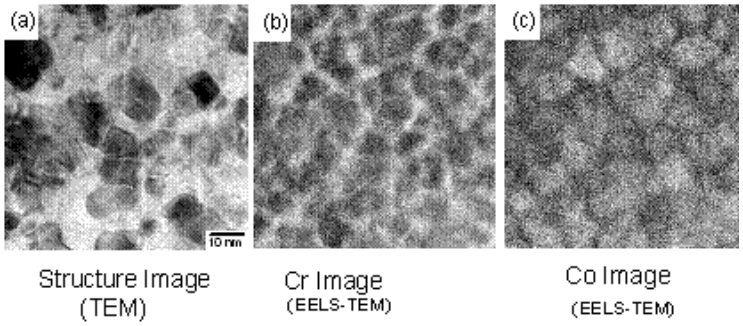

Fig. 6. Plan-view microstructure of $CoCr_{15}Ta_4$ longitudinal thin film observed by EELS-TEM: (a) Zero-loss TEM image (b) Cr-core loss image, and (c) Co-core loss image [16].

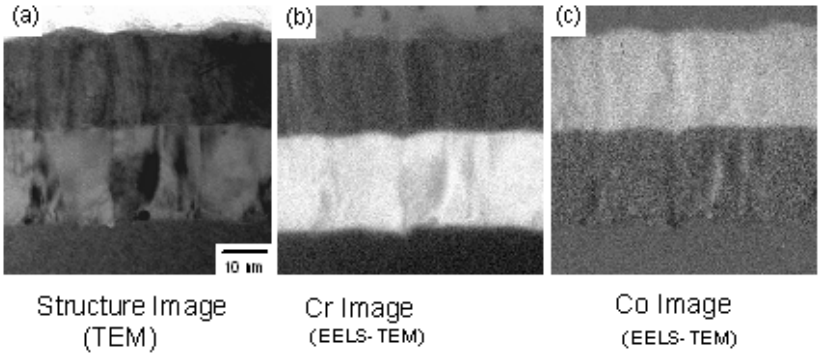

Fig. 7. Cross-sectional microstructure of $CoCr_{15}Ta_4$ longitudinal thin film observed by EELS-TEM: (a) Zero-loss TEM image, (b) Cr-core image, and (c) Co-core loss image [16].

3. Compositional analysis by TEM equipped with EDX

3.1 CoCr-alloy thin film media

A Co-15at%Cr-4at%Ta longitudinal medium sputter deposited at 300 C on a 25 nm-thick Cr-10at%Ti underlayer was also investigated by using a TEM equipped with EDX [19, 21]. A focused electron beam of about 1.5 nm in diameter was used to measure the EDX spectra along the line shown in the plan-view TEM micrograph of Fig. 8 (a). Fig. 8(b) shows the local compositions including the two crystal grain boundaries measured for Co, Cr, and Ta elements. The sample position was carefully selected under the TEM microscope so that the grain boundaries were as parallel to the incident electron beam as possible in order to measure the grain boundary composition accurately. When the grain boundary is slanted with respect to the incident electron beam, the EDX spectrum tends to include chemical composition of crystal grains. From the elements' intensities shown in Fig. 8(b), the Cr concentration at grain boundaries is estimated to be 23 – 26 at% while that inside the grain is fluctuating between 6 and 12 at%. The Co distribution shows the opposite tendency of that of Cr. The Ta seems to show similar tendency with that of Cr, though the accuracy is not high enough to confirm it due to the small amount of only 4at%. The Cr enriched grain boundary width is estimated to be 1.5 – 2 nm by taking into account the electron beam diameter and the angle of incident electron beam. Also based on a careful analysis, the Cr content at the grain boundary is considered to be exceeding 25 at% above which ferromagnetic property begins to disappear. From such detailed analysis, a compositional structure model of CoCrTa medium was proposed [12, 20] which has been used to discuss the magnetic properties through computer simulations.

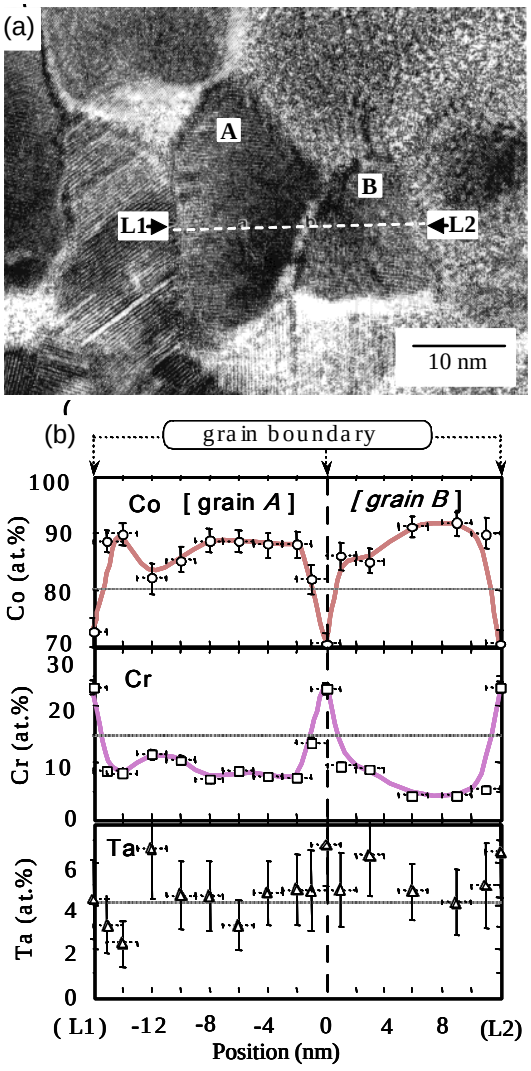

Fig. 8. Plan-view high resolution TEM micrograph of a Co-15.2at%Cr-4.3at%Ta longitudinal thin film medium (a) Variations of Co, Cr and Ta elements along the line L1-L2 mesured by EDX-TEM (b) [20].

Effects of alloy element of Pt on the compositional microstructure was investigated by using a Co-15at%Cr-12at%Pt medium and a Co-14at%Cr-12at%Pt-4at%Ta medium prepared under similar sputtering conditions [23]. The results are shown in Figs. 9 and 10, respectively. The Cr concentration at grain boundary is 5% larger than that of the average value of the CoCrPt medium, whereas it is 4% higher than that of the average value of the CoCrPtTa medium.

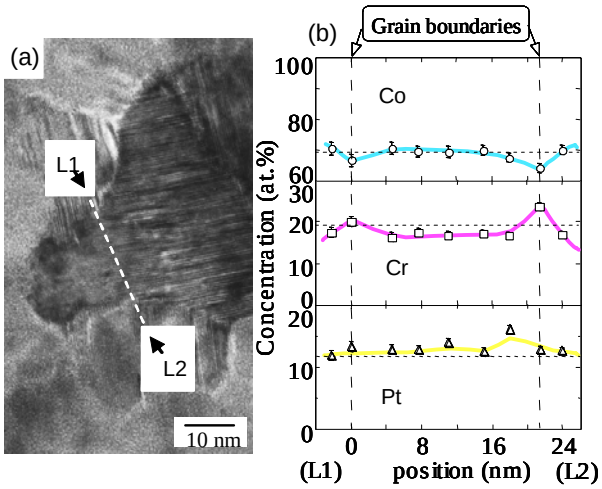

Fig. 9. Plan-view high resolution TEM micrograph of a Co-19at%Cr-12at%Pt longitudinal thin film medium (a). Variations of Co, Cr, and Pt elements along the line L1-L2 (b) [23].

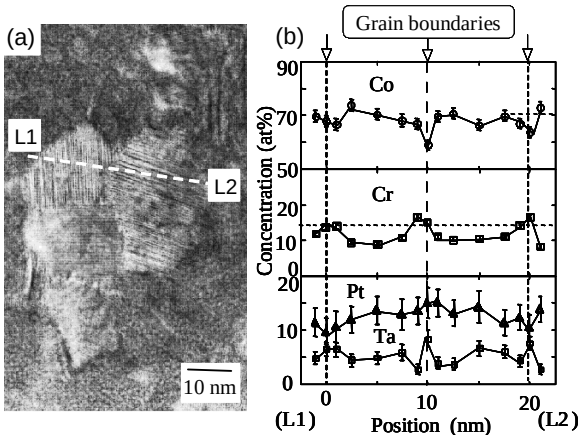

Fig. 10. Plan-view high resolution TEM micrograph of a Co-14%Cr-12at%Pt-4at%Ta longitudinal thin film medium (a). Variations of Co, Cr, Pt, and Ta elements along the line L1-L2 (b) [23].

These results indicate that addition of Pt to Co-alloy thin film does not enhance but rather suppress Cr segregation, and increases the Cr composition inside the magnetic crystal grains. The difference of Cr segregation at a large-angle crystal grain boundary and at a bi-crystal grain boundary was also investigated by careful TEM analysis for a Co-15at%Cr-6at%Ta longitudinal medium. The result is shown in Fig. 11. The Cr content and the thickness of Cr enriched region are about 23 at% and 1 nm, respectively for the large-angle grain boundary whereas they are about 10 at.% and 2 nm, respectively for the bi-crystal grain boundary. This result indicates that Cr segregation profile varies depending on the grain boundary structure.

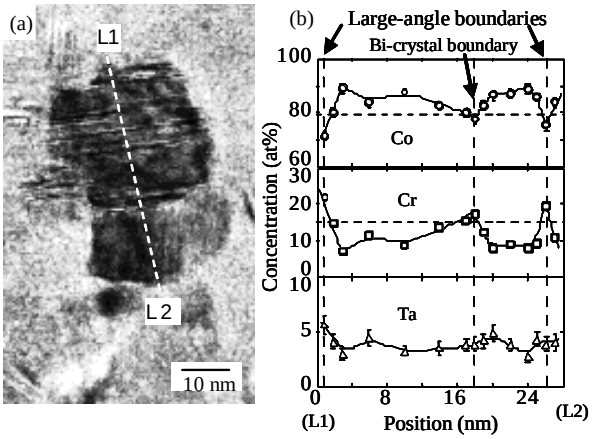

Fig. 11. Plan-view high resolution TEM micrograph of a Co-15.2at%Cr-4.3at%Ta longitudinal thin film medium (a). Variations of Co, Cr, and Pt elements along the line L1-L2 (b). Note the difference of segregation profile between bi-crystalline and large-angle grain boundaries [23].

3.2 Bi-crystal and single crystal thin films

Microscopic compositional structure was investigated for magnetic thin films epitaxially grown on single crystal substrates [23]. Fig. 12 shows the result observed for a bi-crystal Co-15at%Cr-4at%Ta film formed on MgO(100) single crystal substrate employing a Cr-10at%Ti underlayer at a substrate temperature of 300 C. A plan-view TEM micrograph and the Cr distributions are shown in Fig. 12 (b). The electron diffraction showed that the CoCrTa film has the (11.0) growth orientation and consists of two different domains with the c-axis perpendicular each other. Two types of grain boundaries are observed; one is the type where the grain boundary is either parallel or perpendicular to the c-axis of the sub-grains whereas the other is the type where the angle between the grain boundary and the c-axis of sub-grain is 45 degrees. The former type sub-grain boundary shows an enhanced Cr segregation and a narrower width of Cr enriched region than those measured for the latter type sub-grain boundaries. Furthermore, there are Cr compositional fluctuations of around several % within the sub-grains.

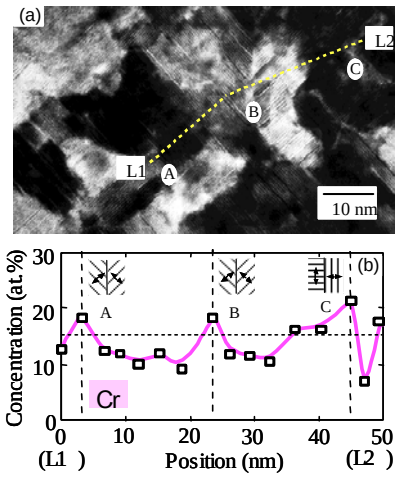

Fig. 12. Plan-view high resolution TEM micrograph of a Co-15at%Cr-6at%Ta by-crystal thin film grown on MgO(100) substrate (a), and Cr atom distribution measured along L1-L2, covering 3 bi-crystal grain boundaries. The inset figures show boundary structures [23].

Compositional structure was further investigated for a single crystal magnetic thin film of Co-19at%Cr-9at%Pt where the addition of Pt is expected to suppress the compositional fluctuation [27, 28]. A 25 nm-thick Co-19at%Cr-9at%Pt layer was deposited on a 50 nm-thick nonmagnetic Co-25at%Cr-25at%Ru layer formed on an Al_2O_3(0001) single crystal substrate by DC-magnetron sputtering at a substrate temperature of 230 C. The cross-sectional TEM micrographs are shown in Fig. 13. The high resolution TEM image clearly indicates that the CoCrPt film is epitaxially grown with the (0001) plane parallel to the CoCrRu(0001) underlayer and the Al_2O_3(0001)substrate. Fig. 13(c) shows the compositional variations of the alloy elements of Co, Cr, Pt, and Ru investigated along sequences of points on two lines for the cross-sectional sample. Compositional fluctuations along the directions of film growth are less than 3 at% for each of the elements in the alloys. Sharp compositional variations of a very few nanometers appear at the interface between the CoCrPtRu and the CoCrPt layers. Fig. 14 shows local concentrations of Co, Cr, and Pt for a plan-view thin film of single crystal CoCrPt(0001) which was extracted from a CoCrPt/CoCrPtRu/Al_2O_3(0001) sample. The film composition was determined as Co71.2 $\pm$ 2.8(2σ) at%, Cr18.0 $\pm$ 2.3(2σ)at%, and Pt 10.8 $\pm$ 1.1(2σ)at%, where σ is the standard deviation. This thin film thus shows slight compositional variation, though it is a (0001)-oriented single crystal. Such compositional fluctuations may occur due to the effect of local stress or strain within the single crystal thin film sample. Compositional fluctuation will readily be enhanced by the presence of crystallographic defects in a Co-alloy sample where the proportion of Cr exceeds the limit of solubility in the phase diagram for the Co-alloy system.

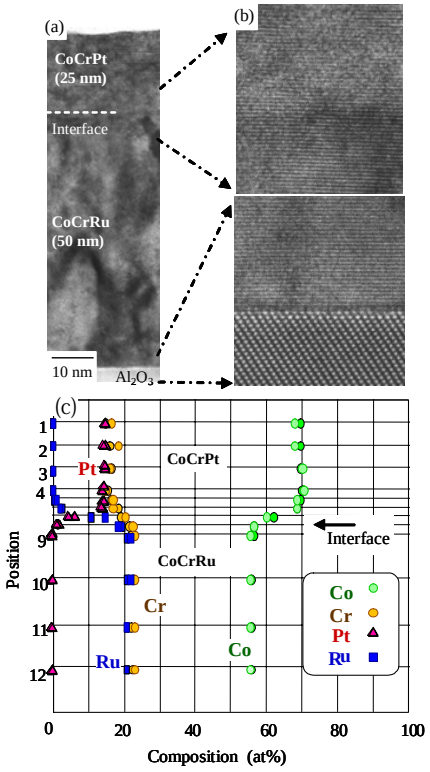

Fig. 13. Cross-sectional TEM micrographs and element distributions of a (0001) oriented single crystal Co-17.7 at%Cr-10.5at%Pt film grown on $CoCr_{25}Ru_{25}/Al_2O_3$(0001) substrate measured along the film grown direction. (a) Cross-sectional TEM, (b) high magnification TEM image of interfaces, and (c) elements distributions measured EDX-TEM [27, 28].

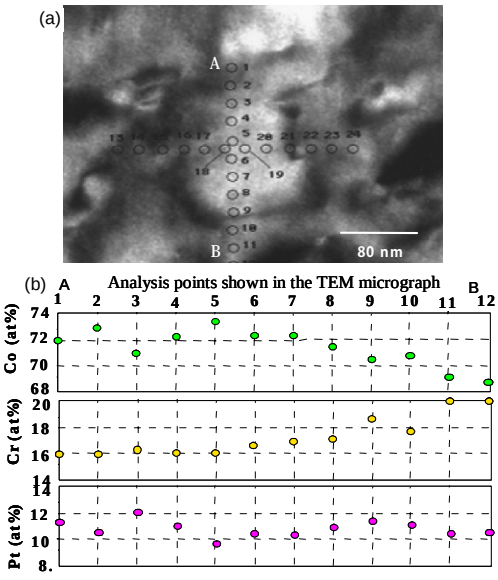

Fig. 14. Plan-view TEM micrograph of a (0001) oriented single crystal Co-17.7at%Cr-10.5at%Pt film thin (a) and variations of Co, Cr, and Pt elements along the line A-B (b). There are compositional fluctuations for the single-crystal thin film [23].

3.3. CoCrPt-SiOx perpendicular thin film media

A compositional analysis using a field emission TEM equipped with an EDX analyzer was applied to a CoCrPt-SiO_x perpendicular medium with granular structure [25, 26]. With this type media, magnetic crystal grains of sub-10 nm in diameter are separated by oxide-based grain boundaries of around 1 – 2 nm width and this type granular media have been used as the recording media of HDD with the areal density greater than 100 Gb/in^2. The number of magnetic crystal grains in a recording bit is less than 100, which implies that the magnetic property of individual crystal grain will directly influence the recording and the thermal stability properties. Plan-view TEM micrographs of the thin film media are shown in Fig. 15. A high magnification TEM image clearly indicates that the grain boundary structure is amorphous. The average metallic composition of the CoCrPt-SiO_x medium determined by using a wide electron beam was 48.2at%Co-10.5at%Cr-17.9at%Pt-23.4at%Si. The oxygen content could not be determined due to a lack of EDX sensitivity.

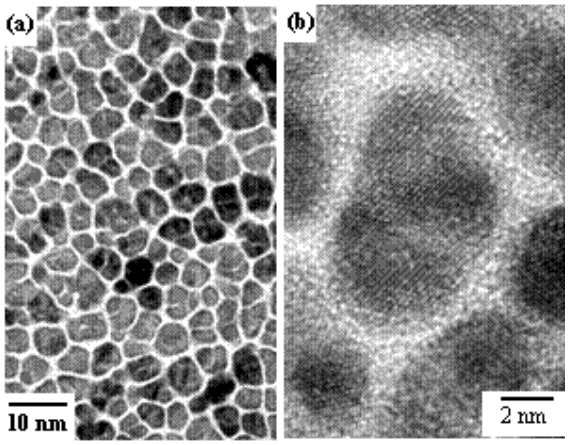

Fig. 15. Plan-view TEM images of CoCrPt-SiO_x medium [26].

Fig. 16 shows the grain diameter distribution measured for the medium, where the crystal grain diameters are distributed around the average value of 7.9 nm with the standard deviation σ = 1.7 nm. The compositions measured for 35 crystal grains using focused electron beam of about 2 nm in diameter are plotted as a function of grain diameter as shown in Fig. 17. The compositions of elements vary depending little on grain diameter, though there are roughly $\pm$ 30 % scatter around the average values indicated by straight lines in the figure. However, the Pt content increases at a very small rate of 0.17 at%/nm, whereas the Si content tends to decrease at a rate of 0.24 at%/nm with increasing the grain diameter, which indicates that the magneto-crystalline anisotropy *(Ku)* increases a little bit with increasing the grain diameter. The average grain boundary composition is estimated by subtracting the grain composition from the average film composition by considering the volume ratio of crystal grains and the boundaries in the film structure [26]. The average grain boundary composition is determined to be 14.4at%Co-17.4at%Cr-12.8at%Pt-55.4at%Si, where Si atoms are expected to exist in a form of oxide, SiO_x. It is notable that not a small amount of other metallic elements seem to be included in the grain boundaries. The composition suggests that the grain boundary is non-magnetic at room temperature.

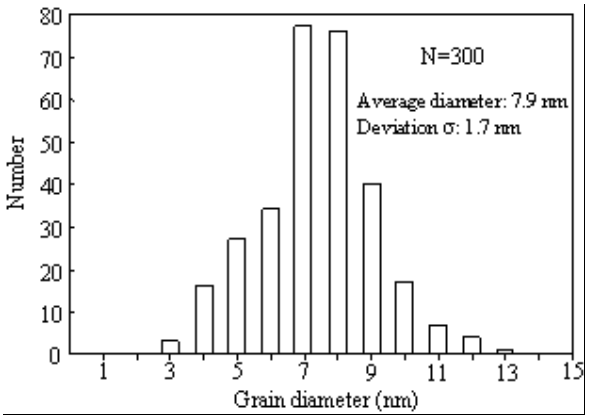

Fig. 16. Grain diameter distribution [25, 26].

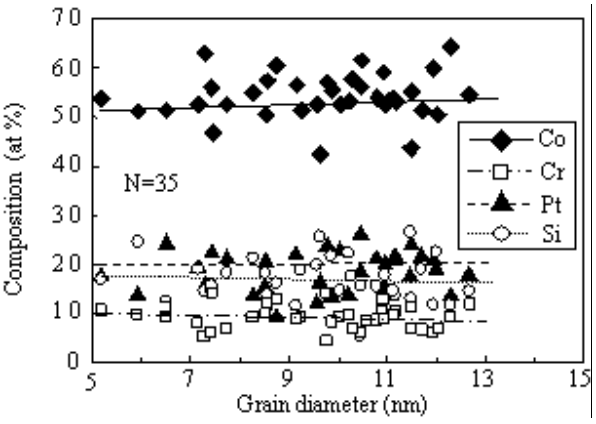

Fig. 17. Magnetic crystal grain compositions of CoCrPt-SiO_x medium investigated by EDX by EDX-TEM [25, 26].

Using the compositions of individual crystal grains, it is possible to roughly estimate the magnetic properties of crystal grains and their distributions. Relationships between the magnetic properties and the composition of CoCrPt-SiO_2 perpendicular media are reported in the references [29, 30]. Under several assumptions like that the Si content determined is related with the SiO_2 composition in the reference neglecting the oxygen situation whether it is in a form of oxide or dissolved in the Co-alloy, it seems useful to correlate the composition of individual crystal grains with the magnetic properties. Fig. 18 shows the *Ms, the Ku,* and the *KuV/kT* dependences on crystal grain diameter of the CoCrPt-SiO_x magnetic recording medium. The thermal stability factor *KuV/KT* is calculated by referring the grain diameter and the thickness (12 nm) for individual crystal grains at

T=300K. The critical grain diameter below which the factor becomes less than 60 is estimated to be 7.6 nm. From the data shown in Figs. 16, 17, and 18, it is possible to quantitatively discuss the crystal grain-level magnetic properties that are very useful to evaluate the microscopic magnetization behavior and the thermal stability behavior of recording media. When the electron beam diameter is further reduced down to below 1 nm, the technology of TEM equipped with EDX will be more effectively used to investigate the sub-nm-level detailed compositional structures of various magnetic thin films.

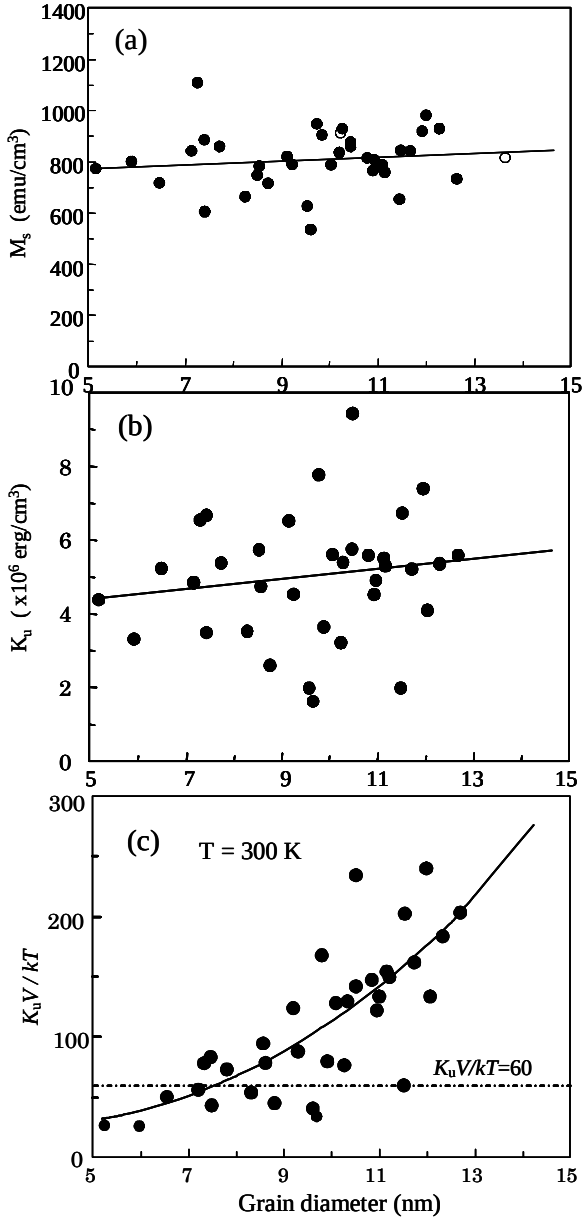

Fig. 18. Magnetization (M_s), magnetic anisotropy energy (Ku) value distributions of CoCrPt-SiO_x medium crystal grain plotted as a function of grain diameter (a), (b). KuV/kT values are estimated at T=300 K for individual crystal grains (c) [25, 26].

4. Summary

Transmission electron microscopy (TEM) has been applied to investigate the detailed microstructure under high special resolution conditions. When a chemical analysis technique using electron energy loss spectroscopy (EELS) or energy dispersive X-ray spectroscopy (EDX) was combined with TEM, it became possible to study both the detailed compositional and the structural information which are necessary to understand the basic magnetic properties of thin films. The applications of such TEM-based technologies on magnetic thin films are reviewed covering the research works carried out from middle 80's to the present. Examples of nm-level chemical analysis are shown for various Co-alloy thin films; polycrystalline, highly oriented, bi-crystalline, and single crystalline thin films. An example of quantitative chemical analysis is also shown for current CoCrPt-oxide granular-type perpendicular media used in commercial hard disk drives. Such quantitative data are believed to be useful not only for understanding the basic magnetic properties but also inevitable for designing the microstructure of future thin film materials.

References

[1] R. Sugita, T. Kunieda, and F. Kobayashi, IEEE Trans. Magn. **MAG-17,** 3172 (1981).
[2] F. Bolzoni, F. Leccabue, R. Pannizzieri, L. Pareti, J. Mag. Mag. Mater. **31-34**, 845(1983).
[3] Y. Maeda, S. Hirono, M. Asahi. Jpn. J. Appl. Phys., **24**, L951 (1985).
[4] Y. Maeda, M. Asahi, J. Appl. Phys. **61**, 1972(1987).
[5] Y. Maeda, D. J. Rogers, O. Song, K. Takei, T. Ohkubo, S. Hirono, J. Suzuki, Y. Mori, IEEE Mag. **33**, 879 (1997).
[6] H. Suzuki, N. Gonda, S. Narishige, Y. Shiroishi, N. Shige, a N. Tsumita, IEEE Trans. Magn. **MAG-27**, 4718 (1991).
[7] K. Yoshida, K. Imagawa, F. Kugiya, H. Daimon, S. Yamagata, O. Kitakami, H. Yasuoka, J. Mag. Soc. Jpn., **13**(S1), 425 (1989).
[8] J. N. Chapman, I. R. McFayden, J. P. C. Bernards, J. Mag. Mag. Mater. **62**, 359 (1986).
[9] D. J. Rogers, J. N. Chapman, J. P. C. Bernards, S. B. Luitjens, IEEE Trans. Magn. **25**, 4180 (1989).
[10] K. Kimoto, Y. Yahisa, T. Hirano, K. Usami, S. Narishige, Jpn. J. Appl. Phys. **34**, L352 (1995).
[11] K. Kimoto, Y. Hirayama, M. Futamoto, J. Mag. Mag. Mater. **159**, 401(1996).
[12] M. Futamoto, N. Inaba, Y. Hirayama, K. Kimoto, K. Usami, Tech. Rep. IEICE **MR95-49**, 35(1995-11).
[13] Y. Hirayama, M. Futamoto, K. Kimoto, K. Usami, IEEE Trans. Mag. **32**, 3807(1996).
[14] M. Futamoto, Y. Hirayama, Y. Honda, K. Ito, K. Yoshida, J. Mag. Soc. Jpn. **21**(S2), 141 (1997).
[15] M. Futamoto, N. Inaba, Y. Hirayama, K. Ito, Y. Honad, Mat. Res. Soc. Symp. Proc. **511**, 243(1999).
[16] M. Futamoto, N. Inaba, Y. Hirayama, K. Ito, Y.

Honda, J. Mag. Mag. Mater. **193**, 36 (1999).
[17] J. E. Witting, T. P. Nolan, R. A. Ross, M. E. Schabes, K. Tang, R. Sinclair, J. Bentley, IEEE Trans. Magn. **34**, 1564 (1998).
[18] R. Sinclair, J. Risner, U. Kwon, F. Hussein-Babei, Digests of PMRC 2007, 17aA-02, Oct. 2007.
[19] M. Futamoto, Tech. Rep. IEICE **MR94-81**, 53 (1995).
[20] N. Inaba, T. Yamamoto, Y. Hosoe, M. Futamoto, J. Mag. Mag. Matter. **168**, 222 (1997).
[21] N. Inaba, M. Futamoto, Tech. Rep. IEICE **MR98-64**, 1 (1999).
[22] N. Inaba, Y. Uesaka, M. Futamoto, IEEE Trans. Mag. **36**, 54 (2000).
[23] N. Inaba, M. Futamoto, J. Appl. Phys. **87**, 6863 (2000).
[24] M. Futamoto, Y. Hirayama, N. Inaba, Y. Honda, A. Kikukawa, IEICE Trans. Electron. **E84-C**, 1132 (2001).
[25] T. Handa, Y. Takahashi, R. Araki, M. Futamoto, J. Mag. Soc. Jpn. **32**, 260 (2008).
[26] M. Futamoto, T. Handa, Y. Takahashi, Digests of Intermag-2008, ED-03(2008-5), (submitted to IEEE Trans. Mag.).
[27] M. Futamoto, K. Terayama, K. Sato, Y. Hirayama, IEICE Trans. Electron. **E85-C**, 1733 (2002).
[28] M. Futamoto, K. Terayama, K. Sato, N. Inaba, Y. Hirayama, Mat. Res. Soc. Symp. Proc. **721**, 279 (2002).
[29] T. Shimotsu, H. Sato. T. Oikawa, Y. Inaba, O. Kitakami, S. Okamoto, H. Aoi, H. Muraoka, Y. Nakamura, IEEE Trans. Magn. **40**, 2483 (2004).
[30] T. Shimotsu, H. Sato. T. Oikawa, Y. Inaba, O. Kitakami, S. Okamoto, H. Aoi, H. Muraoka, Y. Nakamura, IEEE Trans. Magn. **41**, 566 (2005).

*Corresponding author: futamoto@ elect.chuo-u.ac.jp